Dynamics of Hydrogen Transfer in Liquids and Solids

Hans-Heinrich Limbach

Volume 9, pp 520–531

in

Encyclopedia of Nuclear Magnetic Resonance
Volume 9: Advances in NMR
(ISBN 0471 49082 2)

Edited by

David M. Grant and Robin K. Harris

Dynamics of Hydrogen Transfer in Liquids and Solids

Hans-Heinrich Limbach

Freie Universität Berlin, Berlin, Germany

The use of NMR spectroscopy as a tool for the study of the dynamics of hydrogen and deuterium transfer in liquids and solids is demonstrated using a number of examples. (1) Single H Transfer dynamics in weak Hydrogen bonds. Example: Kinetic H/D/T isotope effects on the tautomerism of the porphyrin anion in the liquid and the solid state studied by NMR lineshape analysis. (2) Ultrafast Hydrogen Transfer in Hydrogen bonds of medium strength. Example: Solid tetraazaannzulene, studied using ^{15}N CPMAS NMR relaxometry. (3) Triple Proton Transfer in solid Dimethylpyrazole: An example of determination of multiple kinetic isotope effects by ^{15}N CMAS lineshape analysis and magnetization transfer experiments.

1 INTRODUCTION

Hydrogen Transfer and Bonding are important phenomena in biophysical chemistry.[1] Whereas theoretical and laser chemistry have allowed us a deep understanding of these phenomena in the case of isolated molecules and molecular systems our knowledge referring to the liquid state where the majority of chemical and biochemical reactions takes place is much less advanced. This is mainly because different hydrogen bonded species, different local environments and molecular conformations often lead to a lack of resolution in optical and vibrational spectroscopy. On the other hand, high resolution NMR spectroscopy as a 'slow' method sees a molecule in solution as a single entity, where the different environments are averaged out by fast molecular translational and rotational diffusion. Nevertheless, NMR has been always used as a tool for the study of hydrogen bond phenomena, in spite of its limitations. However, many NMR spectroscopists have not yet realized the progress of NMR made in this field in the past decades, which was induced by the general improvement of NMR such as high resolution and dipolar solid state NMR, solid state NMR-relaxation or low-temperature liquid state NMR techniques.

The purpose of this article is, therefore, to review these recent developments using simple introductory examples which are self-explanatory for the NMR-spectroscopists. These examples are taken from my work in the past years. Thus, no attempt is made to give a comprehensive description but rather to give an overall impression of the number of phenomena studied.

One general comment concerning the nomenclature. By NMR we observe either the moving nuclei, i.e., protons, deuterons, tritons which are generally called 'hydrons', or nuclei to which these particles are attached. In the nomenclature of chemistry, hydrons are, however, always bound to heavy atoms, i.e., they do not exist as isolated particles. Therefore, we will often use the term 'hydrogen transfer' instead of proton transfer, if we can not decide whether only a hydron changes place or whether also electrons are moving at the same time which compensate the charge of the proton. We will use the term 'proton transfer' mainly if it is clear that a proton is transferred with its positive charge.

We will start with single and multiple hydrogen transfer processes between nitrogen involving a barrier that will be gradually removed as the N–H- -N hydrogen bond strength is increased. The techniques of line shape analysis, magnetization transfer and longitudinal relaxation are used in order to follow the hydrogen transfer kinetics. Generally, we will exploit the modulation of isotropic chemical shifts associated with the hydrogen transfer, a stratagem which works in the case of liquids and solids, where high-resolution NMR spectroscopy under the conditions of magic angle spinning (MAS) and cross polarization (CP) can be employed.[2] In the case of liquids and hydrogen transfer from and to nitrogen, however, also the modulation of scalar ^{1}H–^{15}N coupling during hydrogen transfer is a very useful phenomenon to exploit.

2 SINGLE H/D/T TRANSFER ALONG WEAK HYDROGEN BONDS

2.1 Example: The Conjugate Porphyrin Anion

In this section we will discuss the elucidation of the kinetics of the tautomerism of the conjugate ^{15}N-labeled porphyrin anion (Por-H$^-$), a process reported by Braun et al.[3,4] which is depicted Figure 1. The anion was prepared by abstraction of a proton from the ^{15}N-labeled parent compound porphyrin (Por-H_2) by the phosphazene base P_4 (Figure 1). The rate constants of the proton transfer k^H in the conjugate porphyrin anion were determined by analysis of the variable temperature NMR signals of the inner proton of in Por-H$^-$ dissolved in THF-d_8 as depicted in Figure 1(a). The signals appear around -2.7 ppm which is typical for porphyrins; for comparison, the corresponding signals of the parent compound appear at -3.5 ppm.[5] At low temperatures, a doublet is observed arising from scalar coupling with the attached ^{15}N nucleus, indicating a slow exchange of the proton between the nitrogen sites. A differential line broadening of the ^{1}H–^{15}N doublet is observed at low temperature and arises from a reduced molecular mobility and an interference between the ^{1}H–^{15}N dipolar interaction and the chemical shift anisotropy.[6] As temperature is increased, rotational diffusion becomes faster and the asymmetry disappears.

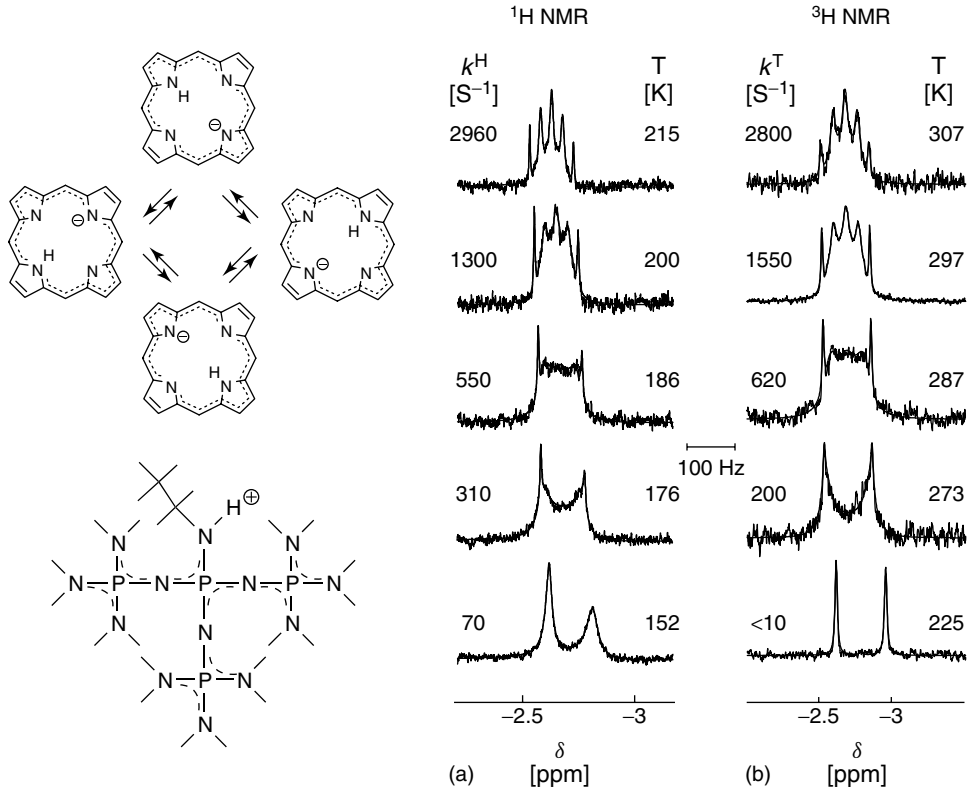

Figure 1 Superposed experimental and calculated variable temperature high field NMR signals of the inner hydrons of the ^{15}N-labeled conjugate porphyrin anion, with the protonated P4-phosphacene base as countercation. Adapted from Braun et al.[4] (a) ^{1}H NMR of a sample containing 65% Por-H$^-$ and 35% Por-D$^-$ dissolved in THF-d_8. Concentration app. 0.015 M; 500 MHz, 65° pulses, duration 6.5 μs, 9 KHz spectral width, 3.5 s repetition time, up to 600 scans. (b) ^{3}H NMR of a sample containing 10% Por-T$^-$ dissolved in THF-h_8; 320 MHz, 5 μs 60° pulses, 8 KHz spectral width, 3.6 s repetition time, number of scans between 200 and 1400 below 250 K and up to 10 000 above 290 K

At the same time, a doublet-pentet transition is observed at about 200 K arising from a fast intramolecular proton transfer between all four nitrogen atoms. The observation of the pentet is proof for an intramolecular reaction pathway of the tautomerism. The rate constants k^H determined by adapting the computed spectra to the experimental spectra corresponds to the inverse average life-time of the proton in a given nitrogen site until either a clockwise or counterclockwise jump to an adjacent nitrogen site occurs, characterized by equal probabilities. No evidence for direct jumps to opposite nitrogen sites were obtained by line-shape analysis as such a process would induce a change of the inner proton signal from a doublet at low to a triplet at a higher temperature. In order to obtain k^H by line-shape analysis the value of the line-width W_o in the absence of exchange is needed. This quantity can be derived at higher temperatures from the line-width of the outer signal components. At low temperatures, where only an exchange broadened doublet is observed, this procedure is not practicable. Here, the signals were simulated by simulating the carbon bound proton signals from which after partial deuteration, also the rate constants k^D are obtained.[4]

In a similar way, the NMR signals of the inner triton of (Por-T$^-$) were measured and analyzed by ^{3}H NMR, and the rate constants k^T of the triton transfer determined, as indicated in Figure 1(b). The doublet-pentet transition temperature is substantially higher for the triton as compared to the proton, indicating a large kinetic H/T isotope effect on the tautomerism.

In order to know the influence of possible cation-anion or other interactions on the tautomerism, variable temperature ^{15}N CPMAS NMR experiments at 9.12 MHz were performed on [Por-H]$^-$ embedded into the phosphacene fluoride depicted in Figure 2. Due to the small magnetic field applied, spinning speeds of between 1.9 KHz and 2.2 KHz were sufficient to suppress the rotational sidebands. At low temperatures, three singlets are observed. exhibiting a ratio of app. 1 : 2.1. The assignment is straightforward: the high-field line arises from the protonated nitrogen, the low-field line from the opposite nitrogen, and the remaining line from the two lateral chemically equivalent nitrogen atoms. As temperature is increased, all lines broaden and coalesce indicating a rapid tautomerism also in the solid state. Moreover, at high temperatures only one single line is observed indicating that the tautomerism renders all nitrogen atoms equivalent. In other words, the gas phase and liquid state degeneracy of the tautomerism is not lifted in the solid matrix. This result is not trivial; although it was also found for the parent compound porphyrin:[5] in most substituted porphyrins the symmetry is lifted by the crystal field.[7]

The line-shape analysis of Figure 2 was carried out in the usual way by setting up the appropriate line-shape equations of intramolecular exchange. The line-width in the absence of exchange were taken from the spectrum at 109 K and the chemical shifts kept constant within the whole temperature range.

The Arrhenius diagram obtained is depicted in Figure 3. Within the margin of error, the rate constants of the proton

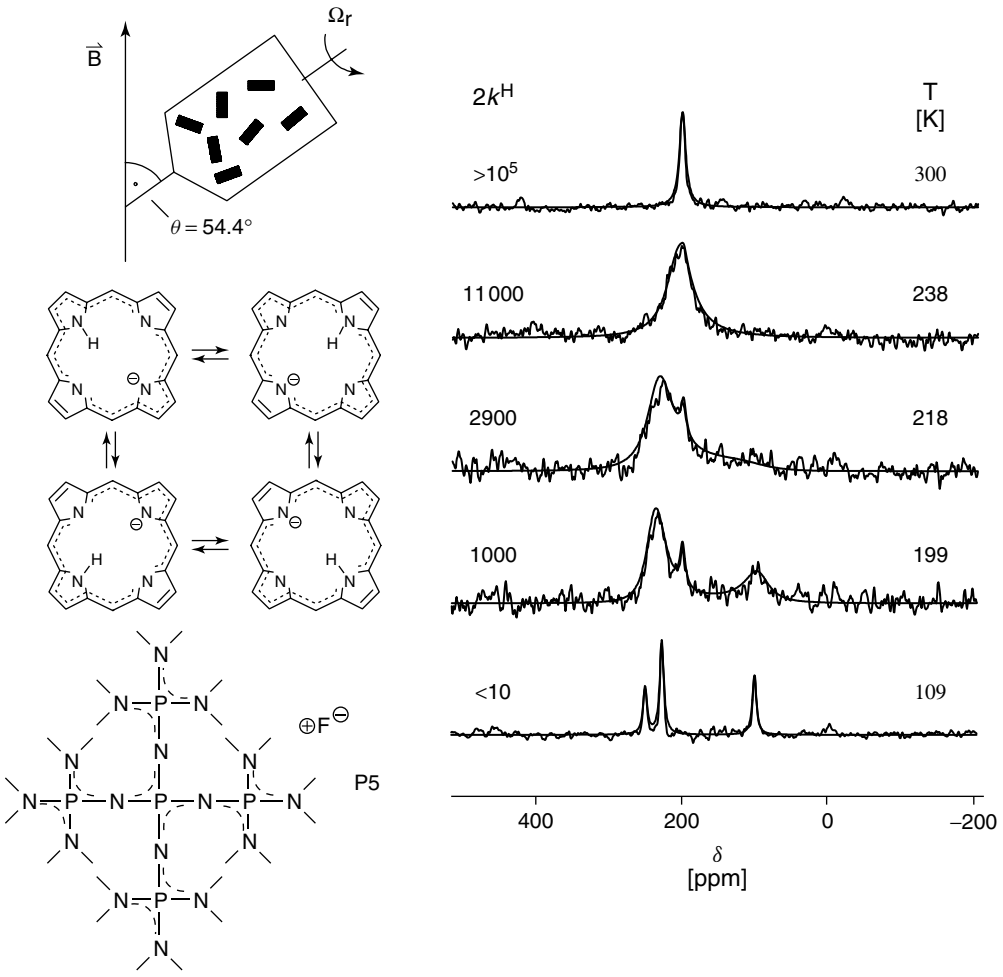

Figure 2 Superposed experimental and calculated variable temperature ^{15}N CPMAS NMR spectra of Por-H$^-$ embedded in solid $P_5{}^+F^-$. 9.12 MHz, 3 to 9 ms CP times, 7 KHz spectral width, 3.3 s repetition time, 1.9–2.2 KHz spinning speed. Flame-sealed glass insert in a 7 mm rotor. The peak labeled with an asterisk arises from an impurity formed during flame sealing. (Adapted from Braun et al.[4])

tautomerism are identical in the liquid and the solid. This means, that in first order the porphyrin skeleton shields the reaction center from the surroundings. The Arrhenius curves of the corresponding processes in the parent compound[5] are also included. We note that especially the proton tautomerism becomes much faster by removing one proton from porphyrin whereas the effect on the D- and the T-transfers are less pronounced. Moreover, the temperature dependence of the rate constants does not follow the Arrhenius law. Together with the large size of the kinetic H/D/T-isotope effects these results indicate a proton tunneling mechanism. This finding is reproduced in terms of a modified Bell[8] tunnel model for both systems.[4] For the parent porphyrin, the tautomerism is stepwise and the transfer of the first proton leads to a metastable intermediate (Figure 3). Proton tunneling cannot occur below the energy of this intermediate. By contrast, in the anion the single proton transfer is degenerate, and tunneling can occur at lower energies. As this phenomenon is very dependent on the mass, it follows that the H-transfer in the anion is especially accelerated as compared to the D- and the T-transfer.

Vangberg et al. have performed ab initio calculations on the tautomerism of the anion.[9] This surface was used by Brackhagen et al.[10] in order to formulate a quantum-mechanical description of the H/D/T-tautomerism. By adapting the calculated set of rate constants to the experimental one insight into the details of the tautomerism could be obtained. This example shows already how dynamic NMR can provide kinetic data which can be used in order to calibrate quantum-mechanical reaction models in polyatomic molecules in condensed phases.

3 MICRO- AND NANOSECOND HYDROGEN TRANSFER PROCESSES IN HYDROGEN BONDS OF MEDIUM STRENGTH

3.1 Example: Tetraazaannzulenes

Whereas in the previous section rate constants were obtained by line shape analysis in the millisecond time scale, the relaxation method allows us to obtain rate constants of proton transfer in solids in the micro- to nanosecond timescale. This method can be used for solids where normal rotational diffusion as a source of relaxation is suppressed. The reason is that the dipolar interactions between moving and nonmoving protons are modulated leading to an important source of relaxation in the solid state.[11,12] On the other hand, moving deuterons lead to a modulation of the quadrupole interaction

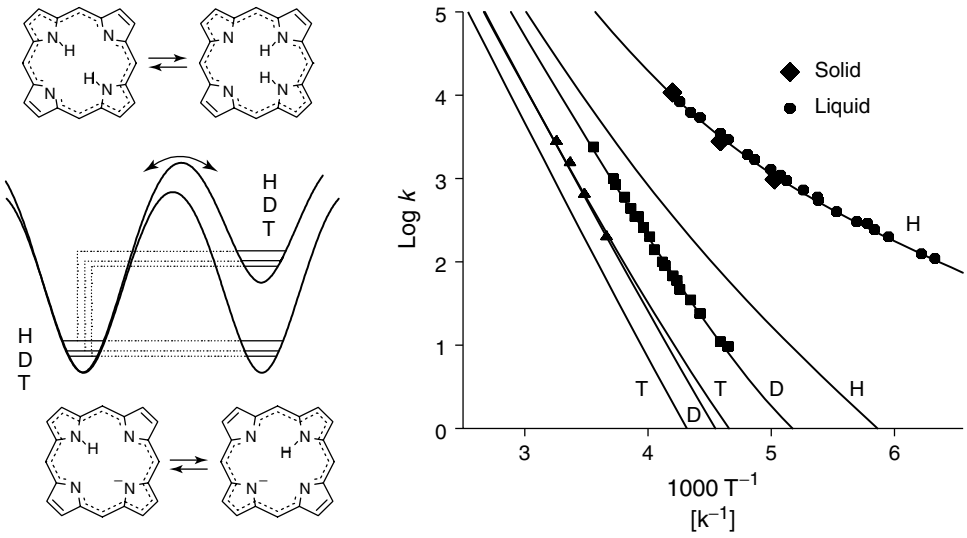

Figure 3 Arrhenius diagram of the H, D, and T transfer in the conjugate porphyrin anion evaluated by dynamic NMR. For comparison, the Arrhenius curves of the parent porphyrin Por-H_2 are included. (Adapted from Braun et al.[4])

and hence to quadrupole relaxation.[13] In order to obtain rate constants of the proton motion it is necessary to know the equilibrium constants. The latter can be obtained in the case of ^{2}H NMR studies but not easily by ^{1}H NMR. Also, the study of polycrystalline powders is difficult.

Finally, we note that the problem can also be overcome by ^{1}H relaxation as a function of the strength of the magnetic field, a method advanced by Horsewill et al.[12]

In the case of proton transfer from and to nitrogen, ^{15}N CPMAS can provide the equilibrium constants in a simple way. By combination with ^{15}N relaxation measurements under CPMAS conditions it is then possible to obtain also the rate constants.

3.2 Dimethyltetraaza[14]annulene (DTAA)

First we will treat the tautomerism of the tetraazaannulene derivative DTAA – discovered by Limbach et al.[14] Hoelger et al.[15] have used this molecule in order to establish the method of ^{15}N longitudinal relaxation under CPMAS conditions and to link it to the technique of line shape analysis, as shown in the following.

In Figure 4(a) are depicted the variable-temperature ^{15}N CPMAS spectra of ^{15}N labeled DTAA. At low temperatures two lines are observed, the high-field line for the protonated and the low-field line for the non-protonated nitrogen. As temperature is increased the lines broaden, but do not coalesce. This situation is typical for an asymmetric situation, where the equilibrium constant of the tautomerism $K = k_{12}/k_{21} = x_1/x_2 < 1$ in the whole temperature range, where k_{12} represents the forward reaction rate constant and x_1 the mole fraction of state **1**, with $x_1 + x_2 = 1$. This leads at high temperatures to two different nitrogen atoms **a** and **b**, where **a** experiences a higher average proton density as compared to **b**. Hence, the chemical shift of **a** at high temperatures is given by

$$\nu_a = x_1\nu_{a1} + x_2\nu_{a2} = \frac{\nu_{a1} + K\nu_{a2}}{1 + K} \tag{1}$$

where ν_{a1} represents the chemical shift of nucleus a in tautomeric state **1**. A similar equation is valid for ν_b from which it follows, that the chemical shift difference at high temperature is given by

$$\delta\nu_{ab} = \nu_a - \nu_a = \Delta\nu_{ab}\frac{1 - K}{1 + K}, \Delta\nu = \nu_N - \nu_{NH} \tag{2}$$

From equation (2) it is easy to obtain the equilibrium constant at high temperatures by comparison of the high and the low-temperature line splittings $\delta\nu_{ab}$ and $\Delta\nu_{ab}$. Once K is obtained at different temperatures it can be extrapolated using the van't Hoff equation to lower temperatures. Then, by line shape analysis rate constants k_{12} can be obtained as indicated in Figure 4(a).

Because of the limited dynamic range the longitudinal ^{15}N relaxation times of ^{15}N labeled DTAA were measured under MAS conditions at 2.1 and 7 Tesla,[15] as indicated in Figure 4(b). For this purpose, the usual sequence of Torchia[16] in connection with CP was employed. A T_1 – minimum was observed around 350 K and 2.1 Tesla. Deuteration of the compound increased the T_1 values strongly, providing evidence that relaxation is caused by the proton jumps that modulate the heteronuclear ^{1}H–^{15}N dipolar coupling. Starting from the homonuclear ^{1}H relaxation theory in the presence of solid state proton transfer[11] equations for the heteronuclear case were derived. It was shown that both nitrogen atoms a and b of a N_a–H- -N_b exhibit the same relaxation times. The latter are normally strongly dependent in the case of a static sample on the orientation of the crystallite with respect to the magnetic field. However, MAS averages out these differences and the relaxation times measured under MAS conditions are almost identical with the isotropic values, which one would obtain for the case of an isotropic rotational diffusion when the latter is not active for relaxation. The final equation used for the data analysis of Figure 4(b) is given by

$$\frac{1}{T_1} = \frac{1}{40}\gamma_N^2\gamma_H^2\left(\frac{h}{2\pi}\right)^2\left(\frac{\mu_o}{4\pi}\right)^2 D\left[\frac{4K}{(1+K)^2}\right] \times \left[\frac{\tau_c}{1 + (\omega_H - \omega_N)^2\tau_c^2} + \frac{3\tau_c}{1 + \omega_N{}^2\tau_c^2} + \frac{6\tau_c}{1 + (\omega_H + \omega_N)^2\tau_c^2}\right] \tag{3}$$

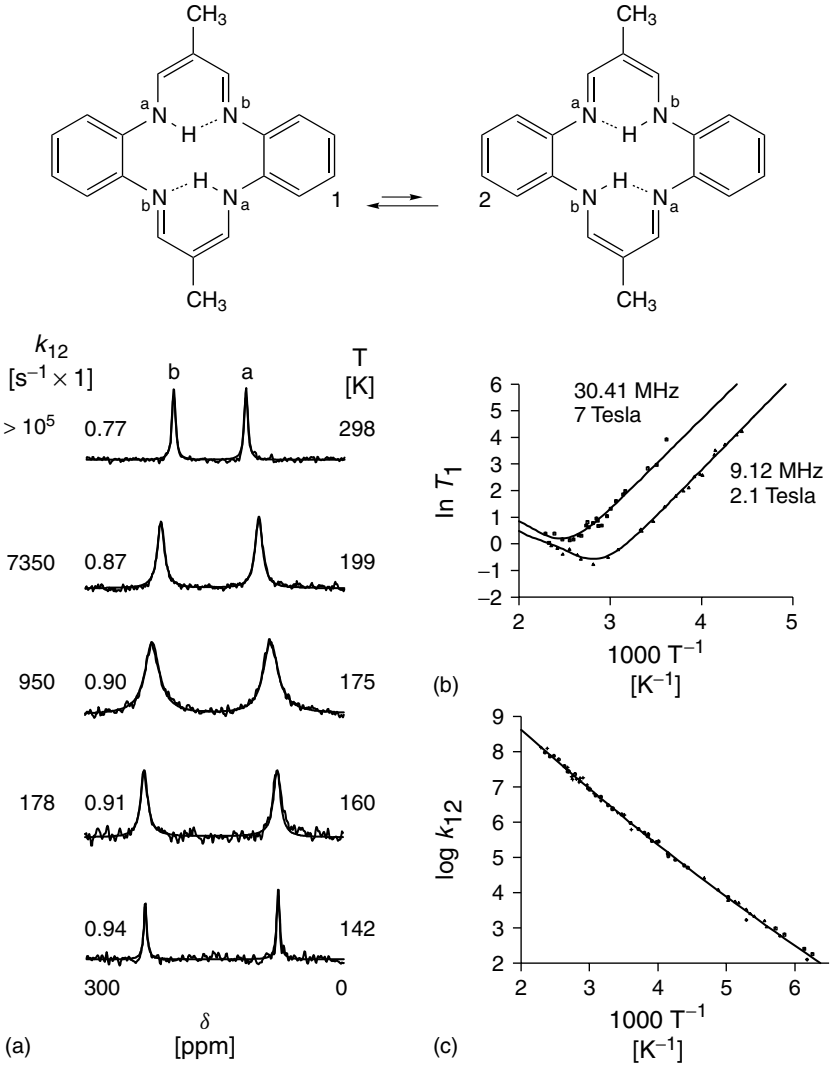

Figure 4 (a) Superposed experimental and theoretical ^{15}N CPMAS NMR spectra of crystalline DTAA. (b) ^{15}N–T_1 analysis. (c) Arrhenius diagram. (Adapted from Hoelger et al.[15])

τ_c is the correlation time of the proton motion whose temperature dependence may be expressed in a first approximation by the Arrhenius equation

$$\frac{1}{\tau_c} = k_{12} + k_{21}, k_{12} = A_{12} \exp\left(\frac{-E_{a12}}{RT}\right) \tag{4}$$

where E_{a12} is the energy of activation of the forward reaction and A_{12} the corresponding frequency factor. The factor D represents the change of the dipolar interaction during the proton jump

$$D = r_1^{-6} + r_2^{-6} + r_1^{-3} r_2^{-3} (1 - 3\cos^2 \theta^d) \tag{5}$$

r_1 represents – for a given nitrogen atom – the short NH distance before and r_2 the long N$\cdots$H distance after the proton has jumped. θ^d represents the angle between the NH vectors before and after the proton transfer, ω represents a Larmor frequency and γ a gyromagnetic ratio.

Using equation (4), the solid lines in Figure 5(b) were calculated using a non-linear least-squares fitting routine, by adapting D – characterizing the T_1 value in the minimum, A_{12} and E_{a12} and assuming an Arrhenius law for the tautomerism. From the value of D it is possible to obtain an approximation of the cubic average short NH-distance $r_1 \equiv r_{NH} = 1.03$ Å which coincides within the margin of error with the value obtained by dipolar NMR for the deuterated compound.[17] Using the parameter set obtained, the relaxation data at 7 Tesla included in Figure 4(b) could be calculated. However, the calculated values were slightly longer than the experimental ones, indicating that at 7 Tesla relaxation via the modulation of the Chemical Shielding Anisotropy by the jumping protons is no longer negligible. Thus, this technique is preferentially performed at lower magnetic fields.

In a second stage of the analysis the assumption of an Arrhenius-law for the proton motion was dropped, and each ^{15}N T_1 value obtained at 2.1 Tesla separately converted into the rate constant k_{12} of the forward proton transfer. The values are plotted together with those obtained by line shape analysis in the Arrhenius diagram of Figure 4(c). The two methods are nearly overlapping, and provide in the overlapping range

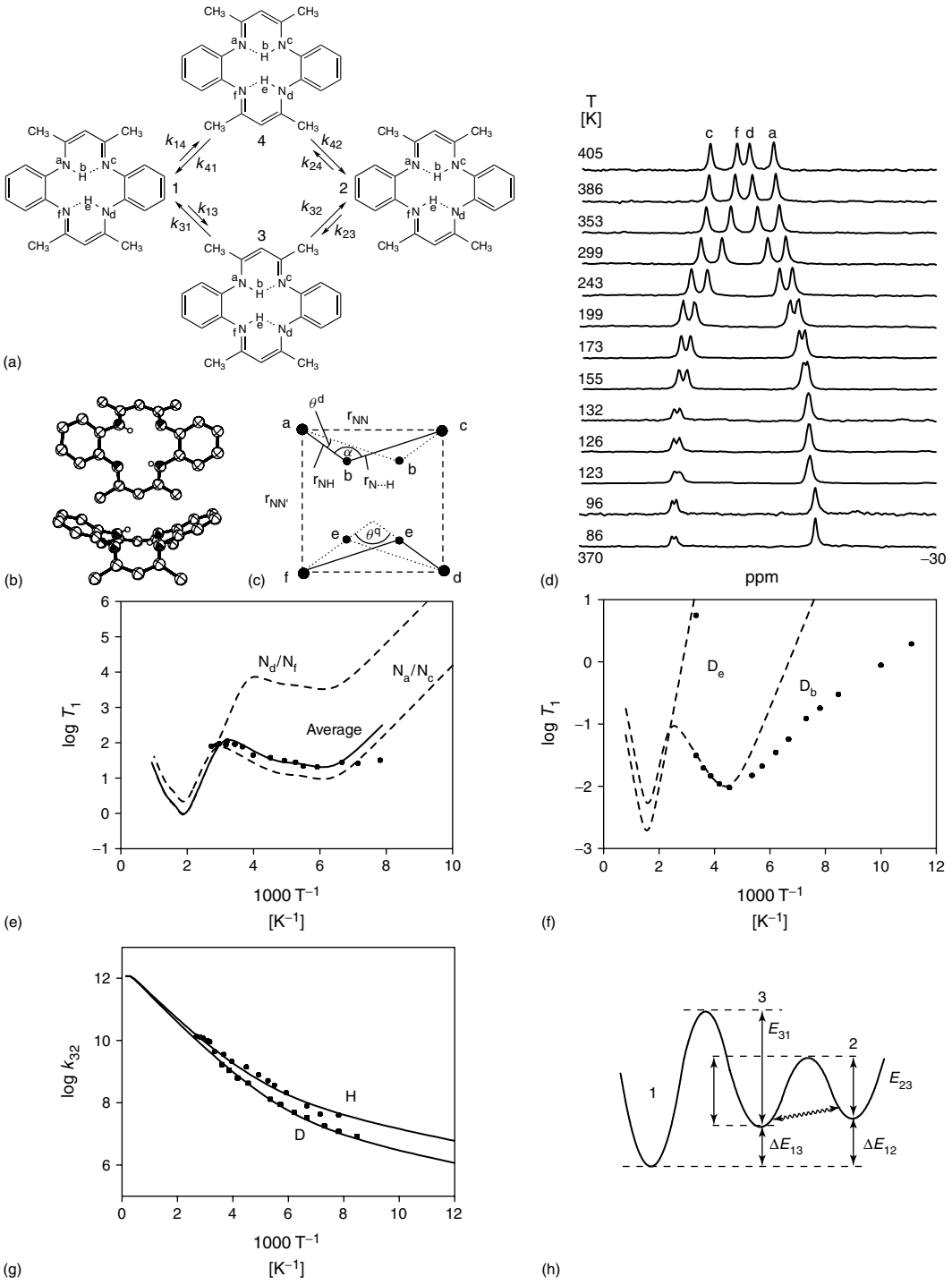

Figure 5 Results of the NMR-experiments on solid TTAA according to Langer et al.[21] (a) The solid state tautomerism of TTAA. (b) Crystal structure of TTAA according to Goedken et al.[19] (c) Geometries of the two intramolecular hydrogen bonds in TTAA, adapted from the crystal structure assuming a planar arrangement. The two positions of each proton are indicated, the angle θ^d is the jump angle of the dipolar ^1H–^{15}N interaction, and α the hydrogen bond angle. θ^q represents the corresponding jump angle of the quadrupole interaction. (d) 9.12 MHz ^{15}N CPMAS-NMR spectra of 95% ^{15}N enriched TTAA at 9.12 MHz as a function of temperature; 6–10 ms cross-polarization time, 7 KHz spectral width, 2.7 s repetition time, 100 scans on average, 2–2.8 KHz rotation frequency (adapted from Wehrle et al.[22]). (e) Temperature dependence of the spin diffusion averaged ^{15}N T_1 relaxation time of polycrystalline TTAA at 9.12 MHz. The solid line was calculated according to equation (3) using the fixed ratios $A_{31}/A_{13} = 1.31$ and $A_{32}/A_{23} = 1.66$ derived in equation (17) and parameter fit of $A_{13} = 1.6 \times 10^{12}\,s^{-1}$, $E_{23} = 14\,KJ\,mol^{-1}$, $E_{31} = 41\,KJ\,mol^{-1}$, and the NH-bond length 1.04 Å. The dashed lines correspond to the intrinsic relaxation times of the nitrogen pairs Na/Nb and Nc/Nd. The T_1 values of the two nitrogen atoms in each pair are identical. (e) T_1 values of deuterons b and e in TTAA plotted in a logarithmic scale as a function of the inverse temperature. (f) Arrhenius diagram of the relaxation active proton and deuteron transfer step **3** $\rightleftharpoons$ **2** of the solid state tautomerism of TTAA. The solid lines were calculated using a modified Bell tunneling model. (h) Energy profile for the double proton transfer in TTAA

similar rate constants which establishes the ^{15}N relaxation method as an important kinetic tool. Rate constants are obtained until the nanosecond time scale. A slight deviation from an Arrhenius behavior is observed, which is, however, less pronounced as in the case of porphyrin and its conjugated anion. This effect was explained again in terms of a stepwise proton motion, where the cis- intermediate exhibits, however, such a high energy that tunneling is not operative.

Finally, we note that the relaxation method discussed here has been recently used in order to obtain the rate constants of the proton motion in the solid porphyrin analog porphycene.[18]

3.3 Tetramethyltetraaza[14]annulene (TTAA)

As an example of the determination of kinetic H/D-isotope effects on the tautomerism we discuss in the following the related TTAA molecule (Figure 5a). Its crystallographic structure is shown in Figure 5(b),[19] and a simplified hydrogen bond structure needed for the interpretation of the relaxation experiments described below in Figure 5(c). The solid state tautomerism of this compound was discovered by Limbach et al.[20] The following results are taken from a recent paper of Langer et al.[21]

The ^{15}N CPMAS spectra of the polycrystalline powder obtained at 2.1 Tesla exhibit four sharp lines a, c, d, and f in the whole temperature range between 86 and 405 K, as depicted in Figure 5(d), with the line separations $\delta_{ac} = \delta_a - \delta_c$ and $\delta_{df} = \delta_d - \delta_f$. This result indicated four chemically inequivalent nitrogen atoms exhibiting different temperature-dependent proton densities. By performing so-called 'spin diffusion' experiments discussed in a later section it was shown that each molecule in the asymmetric unit contains all types of nitrogen atoms. This result is then only consistent with the presence of more than two tautomeric states, i.e., with a stepwise proton transfer mechanism. In other words, in contrast to DTAA, the energy of the cis-intermediate must be substantially lowered. Deuteration of the inner proton sites did not affect at all line positions. This means that there are no H/D-isotope effects on the proton transfer equilibria of solid TTAA. A careful analysis of the splittings δ_{ac} and δ_{df} in terms of the reaction network of Figure 5(a) showed that only states **1**, **2** and **3** are populated but not state **4**.[22] Furthermore, the energy differences between the states could be obtained.

In order to analyze the ^{15}N T_1 values obtained at 9.12 MHz of Figure 5(e) as a function of temperature – which exhibited only a very small and puzzling temperature dependence – we needed to extend the ^{15}N relaxation theory to the two-step proton transfer $\mathbf{1} \rightleftarrows \mathbf{3} \rightleftarrows \mathbf{2}$ and to have an idea of the exact hydrogen bond geometry which was obtained in approximation as follows as no neutron diffraction study of TTAA was available. Knowing the array of the nitrogen atoms from the crystal structure, we assumed that the hydrogen atoms are located in the plane of this array, and that the short NH distances r_{NH} and the long NH-distances $r_{H\cdots N}$ distances are the same for all hydrogen bonds in all tautomers. First we set $r_{NH} = 1.03$ Å which is within the margin of error identical with the value of 1.04 Å obtained by dipolar relaxometry and dipolar ND – coupling for the related DTAA molecule.[17] The slightly smaller value was later justified by a least squares fit of the relaxation data. Knowing the short N–H distance, we made use of the well-known correlation between r_{NH} and $r_{H\cdots N}$ of NHN–Hydrogen bonds established by neutron diffraction,[23] NMR and theoretical calculations,[24] from which we obtained a long N···H distance of 1.94 Å. Taking into account the crystallographic distance of $r_{NN} = 2.675$ Å between the two nitrogen atoms of a given hydrogen bond and of $r_{NN'} = 2.699$ Å between closest nitrogen neighbors in different hydrogen bonds,[19] we derived then the proton positions of Figure 5(c), exhibiting a hydrogen bond angle of $\alpha = 134°$, a dipolar proton jump angle of $\theta^d = 13.7°$, and a quadrupolar jump angle of $\theta^q = 104°$.

With this parameter set, the individual T_1 values of all nitrogen atoms could be calculated, and hence the value of all nitrogen atoms, averaged by spin diffusion. The energy profile for this motion is depicted in Figure 5(h). The agreement between the calculated and experimental values is very satisfactory. The theory predicts two minima, one at low temperatures for the fast process $\mathbf{3} \rightleftarrows \mathbf{2}$ and one at high temperatures, arising from the process $\mathbf{1} \rightleftarrows \mathbf{3}$. As in the fast process only H_b is jumping between N_a and N_c, only these two atoms should experience a short relaxation time at low temperatures, but not N_d and N_c. However, spin diffusion averages this difference.

Independent evidence for this interpretation could be obtained by ^2H NMR relaxation time measurements of the static deuterium labeled solid, where the results are depicted in Figure 5(f). Effectively, two deuterons were observed at room temperature exhibiting different relaxation times, a short one (31 ms) attributed to D_b and a very long one (5.6 s) attributed to D_e.

In the final step, the ^{15}N T_1 values could be converted to the rate constants k_{32}^H and the ^2H T_1 to k_{32}^D. The Arrhenius diagram is depicted in Figure 5(g). As compared to DTAA, the process is much faster which we attributed to the more symmetric profile of the reaction, in a similar way as in the porphyrin anion case. Tunneling is pronounced as the Arrhenius curves exhibit a strong curvature. The kinetic H/D isotope effects are much smaller than in the porphyrin anion. These results may provide again input data for computational studies of this reaction.

Finally, we note that TTAA is not only interesting from the standpoint of theory but also from a practical view, as it provides a very convenient chemical shift thermometer for ^{15}N CPMAS measurements.[22] Temperature control in MAS is very important as spinning can strongly increase temperature.[22] An example of its use will be reported in a subsequent section.

3.4 The Tautomerism of TTAA in a Glassy Polystyrene Matrix

The observation that intermolecular interactions perturb the symmetry of a proton transfer system can be rationalized in the scenario of Figure 6. When a bistable molecule exhibiting a symmetric double well for the proton motion in the gas phase is placed in a molecular crystalline environment, the crystal field will induce an energy difference ΔE between the tautomers (Figure 6b), whereas ΔE will be the same for all molecules in a crystal and ΔE will depend in a disordered system such as a glass on the local environment, leading to a distribution of ΔE-values (Figure 6c). At the glass point, some environments may become mobile leading to an average value of $\Delta E_{av} = 0$, whereas other environments still experience non-zero values.

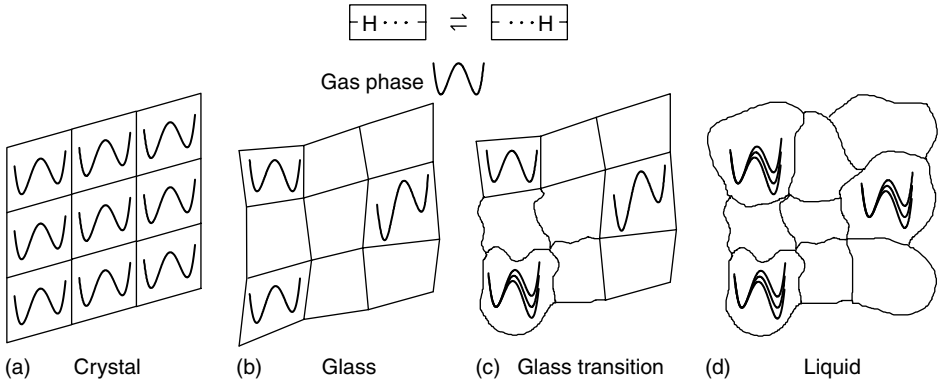

Figure 6 Model for the dependence of the proton transfer potential on the environment arising from experimental observations. (Adapted from Wehrle et al.[25])

Only well above the glass transition is a situation typical for the liquid reached where all molecules exhibit an average value $\Delta E_{av} = 0$ (Figure 6d).

In the case of N–H- -N proton transfer systems the ^{15}N CPMAS line shape for the sequence of Figure 5 has been described, and experimentally verified using the example of TTAA dissolved in solid polystyrene.[25]

3.5 Triple Proton Transfer in Solid Dimethylpyrazole: An Example of Determination of Multiple Kinetic Isotope Effects by ^{15}N CMAS Lineshape Analysis and Magnetization Transfer Experiments

In this section we will introduce three complications, i.e., the problem of the determination of kinetic isotope effects in multiple proton transfer reactions, the case of slow proton dynamics, and the use of the chemical shift thermometer TTAA. In previous liquid state NMR work, we have determined kinetic HH/HD/DD isotope effects of the double proton transfer between acetic acid and methanol already in 1984.[26] However, only in this year, has this process has been modeled a priori.[27] In addition, multiple kinetic isotope effects have been measured for diarylaamidines,[28] which represent the nitrogen analogs of carboxylic acids. The solid state tautomerism of this class of compounds has been reported recently.[29] These studies are still underway. Therefore, as an example, we will treat here the triple proton transfer in solid 3,5-dimethylpyrazole (DMP) (Figure 7a), a process described by Elguero et al.[30] The following results are taken from the paper of Aguilar et al.[31]

The X-ray crystal structure (Figure 7b) shows that this molecule forms a cyclic trimer in the solid state, with half protons close to each nitrogen atom. X-ray diffraction can, however, not distinguish between a 'dynamic disorder' where each molecule can form both tautomeric states to a comparable extent and a 'static disorder' with alternate fixed proton positions from one molecule to the other. The ^{15}N CPMAS spectra of DMP and of its deuterated analog obtained at 7 Tesla with fast speed spinning in order to avoid spinning sidebands are depicted in Figure 7(c) and (d). At low temperatures, two signals are observed for the amino-(–NH–, –ND–) and imino-(–N=) nitrogen atom sites. The cross polarization times used in the experiments were adjusted in such a way that the signals of the amino and imino nitrogen atoms sites were equal. As temperature is increased, the lines broaden and coalesce. As we know from the crystal structure that the molecule forms cyclic trimers, the dynamic process averaging the two isotropic ^{15}N chemical shifts can only correspond to a triple proton transfer. At high temperatures, only a single sharp line survives. This observation indicates that within the margin of error the transfer is degenerate. The coalescence temperature of the deuterated sample is much higher than for the protonated sample and is not reached at 7 Tesla within the temperature range where the compound is solid and indicates the presence of large primary isotope effect k^{HHH}/k^{DDD} on the tautomerism. To the sample of Figure 7(c) a small amount of TTAA was added whose four lines (see Figure 5d) give information about the sample temperature. Thus, line shape analysis of the DMP signals using the usual two-site theory and simulation of the TTAA line positions give both the rate constants as well as the sample temperature, which is increased substantially as compared to the temperature of incoming nitrogen gas by fast MAS. Some rate constants k^{HHD} and k^{HDD} of the other isotopic reactions were obtained by ^{15}N CPMAS NMR line shape analyses of spectra obtained for partially deuterated samples at 2.1 Tesla.

Since at low temperatures the reaction rates are too small to be determined accurately enough by lineshape analysis, one-dimensional ^{15}N CPMAS magnetization transfer experiments in the laboratory frame between the amino nitrogen magnetization S and the imino nitrogen magnetization frame were performed at low temperatures, using a pulse sequence described previously.[32] In these experiments S and X are created by cross polarization and stored by 90° pulses parallel to the magnetic field B_o. The time dependence during this period is monitored after application of a second 90° pulse. The dependence is given by

$$S + X = (S_o + X_o)\exp(-\rho t),\ S - X = (S_o - X_o)\exp\left(-\left(\frac{1}{T_1 + \sigma + 2k}\right)t\right) \qquad (6)$$

where σ represents the rate of spin diffusion between S and X, and k the rate constant of the degenerate triple proton transfer. Two experiments are performed by setting a time interval t_1 between the spin lock pulses and the 90° pulse either to 0 or to $1/2(\nu_S - \nu_X)$, where ν_S and ν_X represent the chemical shifts in Hz of the exchanging sites. In the 'parallel' experiment (i) S_o and X_o have the same sign and are almost equal. Therefore $S - X = 0$ and S and X each decay with the longitudinal

relaxation rate ρ. In the 'antiparallel' experiment (ii) S_o and X_o are antiparallel, i.e., $S_o \approx -X_o$, and each magnetization decays with $\rho + \sigma + 2k$ in time. As ρ is already known from experiment (i) the sum $\sigma + 2k$ is obtained in experiment (ii). Various stratagems have been proposed in order to obtain σ and k separately. Here we exploit the circumstance that σ is strongly dependent on the distance between the ^{15}N nuclei in contrast to k.

As the ^{15}N spin diffusion term σ in equation (6) depends on the internuclear ^{15}N distances, we minimized this term by performing experiments on singly ^{15}N labeled DMP, which reduced the decay constant $\sigma + 2k$ to $2k$ alone; a check by embedding singly ^{15}N labeled DMP into non-labeled DMP at 35% and 10% did not further reduce the observed decay rates.

In Figure 7(e) the results of a typical experiment at a deuterium fraction of $x_D = 0$ and 0.96, carried out at 30.41 MHz and 131 K and spinning speeds of about 8 to 9 KHz i.e., in the regime of suppressed sidebands are depicted. No variation of the magnetizations within the time period covered is observed indicating that $1/T_1$ is so small that it can be neglected. In experiment (ii) performed on the same sample under otherwise similar conditions the two magnetizations cancel each other in the same time period because of the triple proton transfer. For comparison, the results of experiment (ii) on a sample with $x_D \approx 1$ are shown for comparison: no change of the magnetization is observed as the DDD process is very slow. The data analysis (Figure 7e bottom) indicates a mono-exponential from which k^{HHH} is obtained.

In Figure 7(f) are depicted the results of experiment (ii) performed at 210 K on two singly ^{15}N labeled DMP samples with $x_D = 0.2$ and 0.8 are compared. Assuming a statistical isotopic distribution, the ratio for the former sample is given

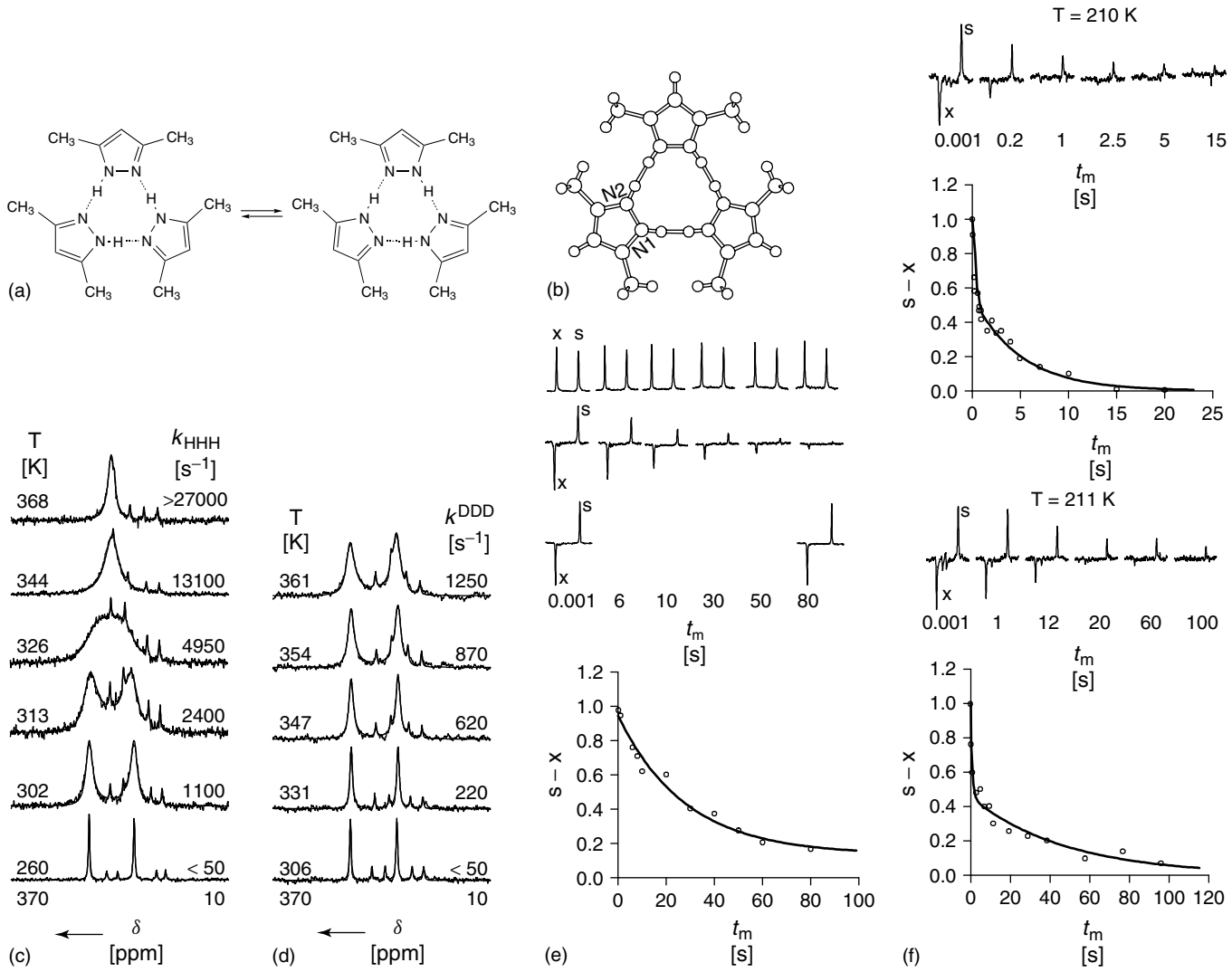

Figure 7 NMR results for the tautomerism of DMP according to Aguilar et al.[31] (a) Triple proton transfer process monitored. (b) X-ray crystal structure of DMP according to Baldy et al.[30a] (c) and (d) Superposed experimental and calculated 30.41 MHz (7 Tesla) ^{15}N CPMAS-NMR spectra of 95% ^{15}N enriched DMP at the deuterium fractions $x_D = 0$ (c) and $x_D = 1$ (d). Experimental conditions: 8–9 KHz sample spinning, 6–12 ms CP times, 4.3 s repetition time, 5 μs ^{1}H 90° pulses. k^{HHH} and k^{DDD} are the rate constant of the triple proton and deuteron transfer. The four sharp lines with temperature dependent line positions stem from a small quantity of the chemical shift thermometer TTAA, added in a separate capsule inside the rotor. (e) 30.41 MHz ^{15}N CPMAS magnetization transfer experiment in the laboratory frame performed on a sample of singly ^{15}N labeled DMP at 131 K. From top to bottom: longitudinal T_1 experiment and magnetization transfer experiment at $x_D = 0$, and MT at $x_D = 0.99$, data analysis for $x_D = 0$. (f) Related experiment at 210 K with $x_D = 0.2$ and $x_D = 0.8$. For further information see text

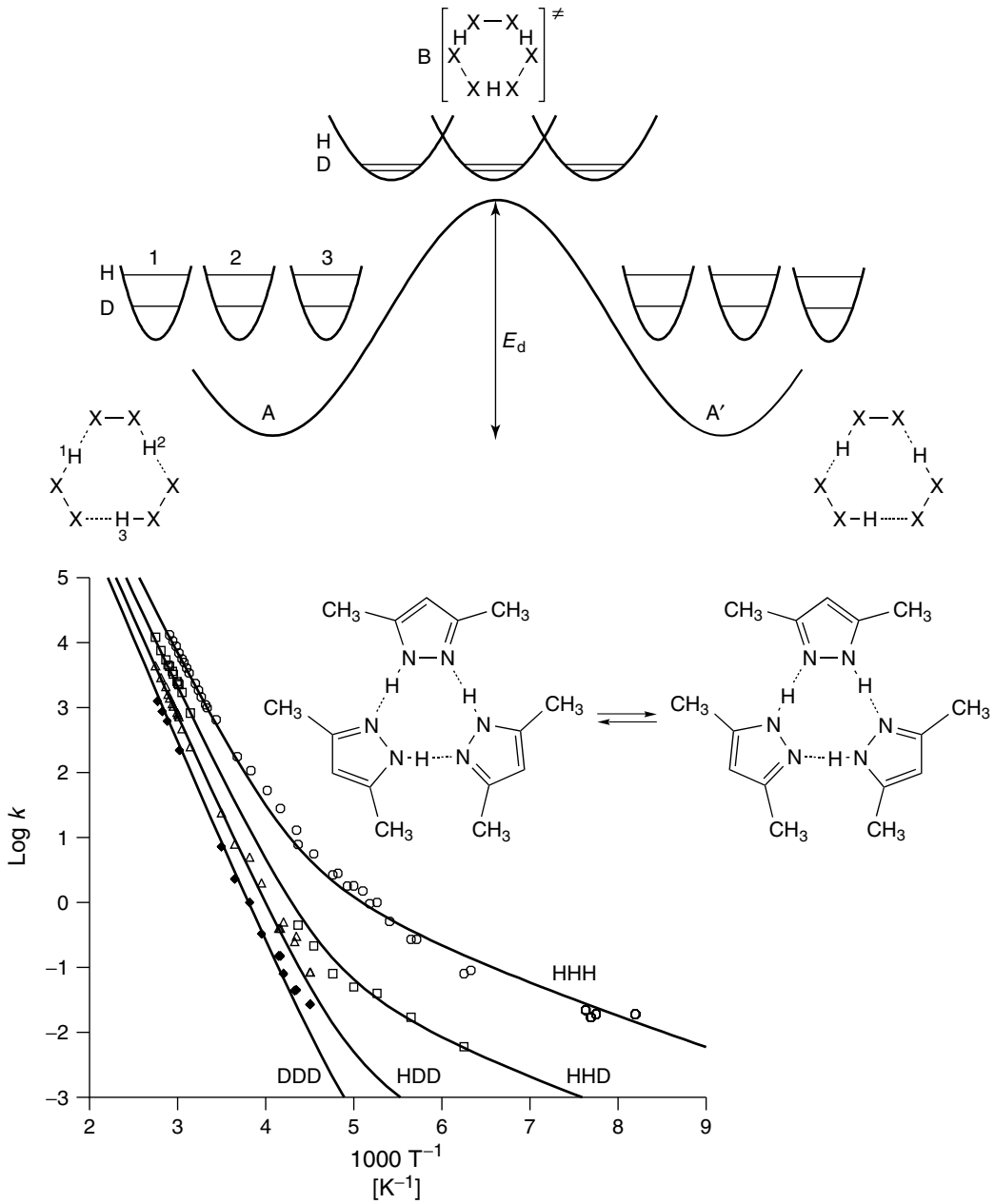

Figure 8 Arrhenius diagram for the triple proton and deuteron transfer in solid DMP according to Aguilar-Parrilla et al.[31]

by $x_{HHH} : x_{HHD} : x_{HDD} : x_{DDD} = 0.512 : 0.384 : 0.096 : 0.08$ and in the second by $x_{HHH} : x_{HHD} : x_{HDD} : x_{DDD} = 0.008 : 0.096, 0.384 : 0.512$. Thus, in the former mainly the HHH and the HHD, and in the latter the HDD and the DDD species dominate, leading to apparently bi-exponential decays in both cases; in the former case the fast and slow decay components are governed by $2k^{HHH}$ and $2k^{HHD}$, and in the second by $2k^{HDD}$ and $2k^{DDD}$. As a consequence the full kinetic HHH/HHD/HDD/DDD isotope effects of the triple proton transfer of DMP could be detected in a large temperature interval.

The Arrhenius diagram containing all the rate constant data for the proton and deuteron transfer in the different DMP species is depicted in Figure 8. Especially in the HHH and the HHD reaction, deviations from a classical Arrhenius behavior were found. The solid lines were calculated in terms of a modified Bell tunneling model as mentioned already in the porphyrin anion case. The interpretation of the data is illustrated at the top of Figure 8. The kinetic data at high temperature indicate that the rule of the geometric mean (RGM) is fulfilled. This rule assumes that all values $k^{HHH}/k^{HHD} \approx k^{HHD}/k^{HDD} \approx k^{HDD}/k^{DDD}$ are equal.[31] Such a case is expected for a concerted triple proton transfer mechanism where all protons loose zero-point energy in the transition state as illustrated in Figure 8. At lower temperatures deviations from the RGM indicate the presence of tunneling. Furthergoing experiments on pyrazole molecules exhibiting a variety of substituents of different size and electronic properties indicated that in the transition state the NHN–Hydrogen bonds are strongly compressed.[33]

4 CONCLUSIONS

In this review, we have demonstrated the use of dynamic liquid and solid state NMR for the study of fast proton and deuteron transfer processes in heterocyclic compounds. The data obtained all indicate the importance of tunneling. They are important for the development of quantum theories of proton transfer and kinetic isotope effects in condensed matter. Techniques have been devised which allow us to use NMR as a tool for the study of proton transfer not only in the second- and millisecond timescale but also in the micro- to nanosecond timescale, if other molecular motions are suppressed as in the solid state.

Naturally, a challenging field opens up when the barrier of proton transfer is further reduced. Then, the realm of H/D isotope effects on hydrogen bond geometries, chemical shifts and coupling constants is reached that provides further details into the phenomenon of hydrogen bonding. This challenging field uses dipolar NMR spectroscopy[24] and low-temperature liquid state NMR techniques.[34] In this realm scalar couplings across hydrogen bonds provide new insight into this phenomenon, if it is possible to reach the slow hydrogen bond exchange regime in the liquid. This is naturally achieved by low temperature NMR methods that also provide information about the influence of the dielectric properties of the solvent on the hydrogen bond geometries. In addition, the technique of isotopic fractionation provides insights into the zero-point energy of hydrogen bonds. This field will be covered in another review that will appear elsewhere. The same is true for the rapidly expanding field of rotational tunnel splittings of hydrogen pairs in transition metal hydrides that give rise to interesting quantum exchange and tunneling phenomena.[35]

5 REFERENCES

1. (a) H. H. Limbach, Dynamic NMR Spectroscopy in the Presence of Kinetic Hydrogen/Deuterium Isotope Effects, in 'NMR-Basic Principles and Progress', Vol. 23, p. 63–164, Springer: Heidelberg, 1991; (b) H. H. Limbach, G. Scherer, L. Meschede, F. Aguilar-Parrilla, B. Wehrle, J. Braun, C. Hoelger, H. Benedict, G. Buntkowsky, W. P. Fehlhammer, J. Elguero, J. A. S. Smith, and B. Chaudret, in 'Ultrafast Reaction Dynamics and Solvent Effects', eds Y. Gauduel and P. J. Rossky, American Institute of Physics, AIP Conference Proceedings 298, 1994, Part III. p. 225–239. NMR Studies of Elementary Steps of Hydrogen Transfer in Condensed Phases; (c) Special Issue 'Hydrogen Transfer; Experiment and Theory', eds H. H. Limbach and J. Manz, *Ber. Bunsenges. Phys. Chem.*, 1998, **102**, 289; (d) Special Issue on 'Proton-Transfer Reactions in Bioenergetics', ed P. Brzezinski, *Biochemica Biophysica Acta – Bioenergetics*, 2000, Vol. 1458.
2. J. Schaeffer and E. O. Stejskal, *J. Am. Chem. Soc.*, 1976, **98**, 1031.
3. J. Braun, C. Hasenfratz, R. Schwesinger, and H. H. Limbach, *Angew. Chem.*, 1994, **106**, 2302; *Angew. Chem. Int. Ed. Engl.*, 1994, **33**, 2215.
4. J. Braun, R. Schwesinger, P. G. Williams, H. Morimoto, D. E. Wemmer, and H. H. Limbach, *J. Am. Chem. Soc.*, 1996, **118**, 11 101.
5. (a) B. Wehrle, H. H. Limbach, M. Köcher, O. Ermer, and E. Vogel, *Angew. Chemie*, 1987, **99**, 914; *Angew. Chem. Int. Ed.*, 1987, **26**, 934; (b) J. Braun, M. Schlabach, B. Wehrle, M. Köcher, E. Vogel, and H. H. Limbach, *J. Am. Chem. Soc.*, 1994, **116**, 6593; (c) J. Braun, H. H. Limbach, P. Williams, H. Morimoto, and D. Wemmer, *J. Am. Chem. Soc.*, 1996, **118**, 7231.
6. (a) H. Shimizu, *J. Chem. Phys.*, 1964, **40**, 3357; (b) H. Rüterjans, E. Kaun, W. E. Hull, and H. H. Limbach, *Nucleic Acids Res.*, 1982, **10**, 7027; (c) R. H. Griffey, C. D. Poulter, Z. Aamaizumi, S. Nishimura, and R. E. Hurd, *J. Am. Chem. Soc.*, 1982, **104**, 5811; (d) M. Gueron, J. L. Leroy, R. H. Griffey, *J. Am. Chem. Soc.*, 1983, **105**, 7262.
7. (a) H. H. Limbach, J. Hennig, R. D. Kendrick, and C. S. Yannoni, *J. Am. Chem. Soc.*, 1984, **106**, 4059; (b) R. D. Kendrick, S. Friedrich, B. Wehrle, H. H. Limbach, and C. S. Yannoni, *J. Magn. Reson.*, 1985, **30**, 159; (c) H. H. Limbach, B. Wehrle, M. Schlabach, R. D. Kendrick, and C. S. Yannoni, *J. Magn. Reson.*, 1988, **77**, 84; (d) M. Schlabach, B. Wehrle, J. Braun, G. Scherer, and H. H. Limbach, *Ber. Bunsenges. Phys. Chem.*, 1992, **96**, 821.
8. (a) R. P. Bell, 'The Tunnel Effect', 2nd edn., Chapman and Hall: London, 1980.
9. T. Vangberg and A. Ghosh, *J. Phys. Chem. B*, 1997, **101**, 1496.
10. O. Brackhagen, Ch. Scheurer, R. Meyer, and H. H. Limbach, *Ber. Bunsenges. Phys. Chem.*, 1998, **102**, 303.
11. (a) A. Stöckli, B. H. Meier, R. Kreis, R. Meyer, and R. R. Ernst, *J. Chem. Phys.*, 1990, **93**, 1502 and references cited therein; (b) S. Takeda, A. Tsuzumitani, and C. A. Chatzidimitriou-Dreismann, *Chem. Phys. Lett.*, 1992, **198**, 316; (c) S. Takeda, T. Inabe, C. Benedict, U. Langer, and H. H. Limbach, *Ber. Bunsenges. Phys. Chem.*, 1998, **102**, 1358.
12. (a) A. J. Horsewill, P. J. McDonald, and D. Vijayaraghavan, *J. Chem. Phys.*, 1994, **100**, 1889; (b) D. F. Brougham, A. J. Horsewill, and R. I. Jenkinson, *Chem. Phys. Lett.*, 1997, **272**, 69; (c) A. J. Horsewill, *Prog. NMR Spectrosc.*, 1999, **35**, 359; (d) A. J. Horsewill, N. H. Jones, and R. Caciuffo, *Science*, 2001, **291**, 100.
13. A. Heuer and U. Haeberlen, *J. Chem. Phys.*, 1991, **95**, 4201; 1991, **187**, 471.
14. H. H. Limbach, B. Wehrle, H. Zimmermann, R. D. Kendrick, and C. S. Yannoni, *Angew. Chem.*, 1987, **99**, 241; *Angew. Chem. Int. Ed. Engl.*, 1987, **26**, 247.
15. C. G. Hoelger, B. Wehrle, H. Benedict, and H. H. Limbach, *J. Phys. Chem.*, 1994, **98**, 843.
16. D. Torchia, *J. Magn. Reson.*, 1978, **30**, 613.
17. C. G. Hoelger and H. H. Limbach, *J. Phys. Chem.*, 1994, **98**, 11 803.
18. U. Langer, Ch. Hoelger, B. Wehrle, L. Latanowicz, E. Vogel, and H. H. Limbach, *J. Phys. Org. Chem.*, 2000, **13**, 23.
19. V. L. Goedken, J. J. Pluth, S. M. Peng Shie-Ming, and B. Bursten, *J. Am. Chem. Soc.*, 1976, **98**, 8014.
20. (a) H. H. Limbach, B. Wehrle, H. Zimmermann, R. D. Kendrick, and C. S. Yannoni, *J. Am. Chem. Soc.*, 1987, **109**, 929.
21. U. Langer, L. Latanowicz, C. Hoelger, G. Buntkowsky, H. M. Vieth, and H. H. Limbach, *Phys. Chem. Chem. Phys.*, 2001, **3**, 1446.
22. (a) B. Wehrle, F. Aguilar-Parrilla, and H. H. Limbach, *J. Magn. Reson.*, 1990, **87**, 584; (b) F. Aguilar-Parrilla, B. Wehrle, H. Bräunling, and H. H. Limbach, *J. Magn. Reson.*, 1990, **87**, 592.
23. Th. Steiner, *J. Chem. Soc. Chem. Commun.*, 1995, 1331.
24. (a) H. Benedict, C. Hoelger, F. Aguilar-Parrilla, W. P. Fehlhammer, M. Wehlan, R. Janoschek, and H. H. Limbach, *J. Mol. Struct.*, 1996, **378**, 11; (b) H. Benedict, H. H. Limbach, M. Wehlan, W. P. Fehlhammer, N. S. Golubev, and R. Janoschek, *J. Am. Chem. Soc.*, 1998, **120**, 2939.
25. (a) B. Wehrle, H. H. Limbach, and H. Zimmermann, *Ber. Bunsenges. Phys. Chem.*, 1987, **91**, 941; (b) B. Wehrle, H. H. Zimmermann, and H. H. Limbach, *J. Am. Chem. Soc.*, 1988, **110**, 7014; (c) B. Wehrle and H. H. Limbach, *Chem. Phys.*, 1989, **136**, 223.
26. D. Gerritzen and H. H. Limbach, *J. Am. Chem. Soc.*, 1984, **106**, 869.

27. A. F. Ramos, Z. Zmedarchina, and J. Rodríguez-Otero, *J. Chem. Phys.*, 2001, **114**, 1567.
28. L. Meschede and H. H. Limbach, *J. Phys. Chem.*, 1991, **95**, 10 267.
29. R. Anulewicz, I. Wawer, T. M. Krygowski, F. Männle, and H.-H. Limbach, *J. Am. Chem. Soc.*, 1997, **119**, 12 223.
30. (a) A. Baldy, J. Elguero, R. Faure, M. Pierrot, and E. J. Vincent, *J. Am. Chem. Soc.*, 1985, **107**, 5290; (b) J. A. S. Smith, B. Wehrle, F. Aguilar-Parrilla, H. H. Limbach, M. C. Foces-Foces, F. H. Cano, J. Elguero, A. Baldy, M. Pierrot, M. M. T. Khurshid, and J. B. Larcombe-McDouall, *J. Am. Chem. Soc.*, 1989, **111**, 7304; (c) F. Aguilar-Parrilla, G. Scherer, H. H. Limbach, M. C. Foces-Foces, F. H. Cano, J. A. S. Smith, C. Toiron, and J. Elguero, *J. Am. Chem. Soc.*, 1992, **114**, 9657; (d) C. G. Hoelger, H. H. Limbach, F. Aguilar-Parrilla, J. Elguéro, O. Weintraub, and S. Vega, *J. Magn. Res.*, 1996, **A120**, 46; (e) O. Klein, M. M. Bonvehi, F. Aguilar-Parrilla, J. Elguero, and H. H. Limbach, *Isr. J. Chem.*, 1999, **34**, 291.
31. F. Aguilar-Parrilla, O. Klein, J. Elguero, and H. H. Limbach, *Ber. Bunsenges. Phys. Chem.*, 1997, **101**, 889.
32. (a) N. M. Szeverenyi, M. J. Sullivan, and G. E. Maciel, *J. Magn. Reson.*, 1982, **47**, 462; (b) H. H. Limbach, B. Wehrle, M. Schlabach, R. D. Kendrick, and C. S., Yannoni, *J. Magn. Reson.*, 1988, **77**, 84.
33. O. Klein, M. M. Bonvehi, F. Aguilar-Parrilla, J. Elguero, and H. H. Limbach, *Isr. J. Chem.*, 1999, **34**, 291.
34. (a) N. S. Golubev, S. N. Smirnov, V. A. Gindin, G. S. Denisov, H. Benedict, and H. H. Limbach, *J. Am. Chem. Soc.*, 1994, **116**, 12 055; (b) S. N. Smirnov, H. Benedict, N. S. Golubev, G. S. Denisov, M. M. Kreevoy, R. L. Schowen, and H. H. Limbach, *Can. J. Chem.*, 1999, **77**, 943. P. Schah-Mohammedi, I. G. Shenderovich, C. Detering, H. H. Limbach, P. M. Tolstoy, S. N. Smirnov, G. S. Denisov, and N. S. Golubev. *J. Am. Chem. Soc.*, 2000, **122**, 12 878. I. Shenderovich, S. Smirnov, G. S. Denisov, V. Gindin, N. S. Golubev, A. Dunger, R. Reibke, S. Kirpekar, O. L. Malkina, and H. H. Limbach, *Ber. Bunsenges. Phys. Chem.*, 1998, **102**, 422. H. Benedict, I. G. Shenderovich, O. L. Malkina, V. G. Malkin, G. S. Denisov, N. S. Golubev, and H. H. Limbach, *J. Am. Chem. Soc.*, 2000, **122**, 1979. N. S. Golubev, I. G. Shenderovich, S. N. Smirnov, G. S. Denisov, and H. H. Limbach, *Chem. Eur. J.*, 1999, **5**, 492.
35. N. S. Golubev, G. S. Denisov, S. N. Smirnov, D. N. Shchepkin, and H. H. Limbach, *Z. Phys. Chem.*, 1996, **196**, 73.
36. (a) H. H. Limbach, S. Ulrich, G. Buntkowsky, S. Gründemann, S. Sabo-Etienne, B. Chaudret, G. J. Kubas, and J. Eckert, *J. Am. Chem. Soc.*, 1998, **120**, 7929; (b) F. Wehrmann, T. P. Fong, R. H. Morris, and H. H. Limbach, Gerd Buntkowsky, *Phys. Chem. Chem. Phys.*, 1999, **1**, 4033.

Acknowledgements

I thank all colleagues that have been coauthors of the papers of our group for their impact on this work. Especially, I thank my coworkers Dr. Gerd Buntkowsky and Dr. Klaus Weisz, Prof. J. Elguero, CSIC, Madrid. This work has been supported by the following sponsors: Deutsche Forschungsgemeinschaft, Bonn-Bad Godesberg, Fonds der Chemischen Industrie, Frankfurt, European Community, Brussels.

Biographical Sketch

Hans-Heinrich Limbach, *b* 1943. Dr. Rer.Nat. 1973, Dr. Habil. 1980, (Physical Chemistry), Universität Freiburg, Germany. Guest scientist with C. S. Yannoni 1983, IBM Research Laboratory, San José, USA, with C. B. Moore, UC Berkeley, 1984. Since 1990 Full Professor of Chemistry, Freie Universität Berlin. Chair Gordon Research Conference Isotopes in the Biological and Chemical Sciences 2002. Editorial Board Magn. Reson. Chem., Spect. Lett., Chem. Phys. Approx 190 publications. Principal research interest: Hydrogen Bond NMR.